JOURNAL OF CATALYSIS 137, 306–321 (1992)

CO Oxidation over Au/ZrO_2 Catalysts: Activity, Deactivation Behavior, and Reaction Mechanism

A. KNELL,* P. BARNICKEL,†,[1] A. BAIKER,* AND A. WOKAUN†,[2]

*Department of Chemical Engineering and Industrial Chemistry, Swiss Federal Institute of Technology, ETH Zentrum, CH-8092 Zürich, Switzerland; and †Physical Chemistry II, University of Bayreuth, D-W-8580 Bayreuth, Germany

Received January 2, 1992; revised April 3, 1992

Gold catalysts supported on amorphous zirconia have been prepared by coprecipitation. These catalysts exhibit a high initial CO oxidation activity, which is due to a synergy between the zirconia and the supported gold particles. The activity decreases significantly over a time scale of ≈20 h. The deactivation behavior is only weakly influenced by pretreatments in O_2, CO, or CO_2. However, the long-time stability is found to depend strongly on the O_2/CO feed ratio. With stoichiometric reaction mixtures (O_2/CO = 0.5), the activity stays nearly constant over the time of observation. In the presence of excess oxygen (O_2/CO = 1 or 40, respectively), rapid deactivation is observed. From a careful monitoring of the carbon balance, and from thermal desorption/mass spectrometry experiments, a progressive covering of the surface by oxygenated carbon species is deduced. Diffuse reflectance FTIR experiments indicate the presence of carbonates, formate, and several types of differently bound CO molecules on the surface. Temperature-dependent experiments reveal that these species are involved in a series of interconnected equilibria, which are coupled to the relevant adsorption/desorption processes. Oxidized and reduced states of the catalyst can be distinguished. The deactivated state in excess oxygen is characterized by a high concentration of surface formate. On the deactivated catalyst, oxydation of formate and of CO appears to be slow, possibly as a consequence of site blocking.

INTRODUCTION

In view of its importance, CO oxidation over solid state catalysts is a subject of intensive investigations (*1*). In the present communication we are focusing on Au/ZrO_2 surfaces for catalyzing CO oxidation. In the past, gold has been less frequently considered as a catalytic material as a consequence of its chemical inertness. More recently, Schwank (*2*) has drawn attention to the potential of gold surfaces as hydrogen and oxygen transfer catalysts.

In 1974, Cant and Fredrickson (*3*) investigated the reaction of CO with oxygen over gold catalysts prepared from gold salts. Schwank (*2*) and Wachs (*4*) reported the use of *supported* gold catalysts for this reaction. The transformation of an amorphous $Au_{25}Zr_{75}$ alloy into an active CO oxidation catalyst has been described by Shibata *et al.* (*5*). The adsorption and oxidation of CO on evaporated and single crystal surfaces has been investigated by a variety of spectroscopic techniques (*6*, *7*).

An upsurge of interest in gold as a catalyst material was triggered by the work of Haruta *et al.* (*8–11*). Over highly dispersed gold catalysts prepared by coprecipitation of gold with a variety of metal oxides, CO oxidation activity at temperatures as low as 200 K has been demonstrated. The authors have pointed out (*9*) that gold is activated for CO oxidation by the interaction with a zirconia support. Group VIII and other transition metal oxides, alkaline earth and Group IIB oxides, Group III and IIIB oxides, as well as SiO_2 and SnO_2, have also

[1] Present address: TÜV Bayern, Westendstrasse 199, D-W-8000 München 21, Germany.

[2] To whom correspondence should be addressed.

0021-9517/92 $5.00

been tested by Haruta *et al.* as carrier materials. Other groups have used yttria (*12*) and ceria/alumina (*13*) as the support oxides. Gardner *et al.* (*14*) observed that the activity of Au/Fe_2O_3 catalysts was strongly reduced in CO_2 rich atmospheres.

In this work gold catalysts supported on amorphous ZrO_2 are investigated. The stabilizing influence of gold on the amorphous state of the zirconia is studied. Various pretreatments in CO, CO_2, O_2, and N_2 are compared, and the influence of the O_2/CO feed ratio is tested with respect to the long-term deactivation behavior of the catalysts. From *in situ* diffuse reflectance FTIR (DRIFT) experiments, information on the mechanism of CO oxidation and the species accumulating on the surfaces of deactivated catalysts are derived.

EXPERIMENTAL

Catalyst Preparation by Coprecipitation

Appropriate amounts of gold chloride ($HAuCl_4$, Johnson Matthey) were added to an aqueous solution of zirconyl nitrate ($ZrO(NO_3)_2$, Johnson Matthey) at 333 K. This solution was added to deionized water at 363–368 K under vigorous stirring, the pH being held constant at a value of ≈7 by NaOH additions. After the precipitation, the fine suspension was aged for 15 min while stirring at 363 K, and then filtered. The solid precipitate was redispersed four times in distilled water and once in methanol. After drying for 15 h at 393 K under reduced pressure and coarse crushing, the catalysts were calcined at 623 K for 5 h. The calcined samples were crushed, and a sieve fraction of 50–150 μm was used for the catalytic tests.

A Cu/ZrO_2 reference catalyst (70 at.% Cu, 30 at.% Zr) was prepared by an analogous coprecipitation procedure at constant pH, starting from $Cu(NO_3)_2$ (Fluka, p.a.).

The Pd/ZrO_2 reference sample (5 wt% of Pd) was prepared by wet impregnation of the amorphous zirconia with an aqueous solution of $(NH_4)_2PdCl_4$. The catalyst was dried at 393 K, calcined, and reduced at 573 K in an H_2/N_2 flow.

Catalyst Characterization

BET surface areas have been determined by means of N_2 physisorption, applying a Micromeritics instrument (Model ASAP 2000), the samples being predried *in vacuo* at 523 K for 5 h.

X-ray diffractograms were recorded in steps of 0.009° (2Θ), using Cu$K\alpha$ radiation, applying a Siemens diffractometer (Model D5000) equipped with a position sensitive detector. The range in 2Θ from 20 to 80° was scanned with an integration time of 5 s/degree. Gold particle sizes were determined using the equation of Warren (*15*).

Thermoanalytic and desorption experiments have been carried out on a Netzsch instrument (Model STA409), coupled through a capillary with a Balzers quadrupole mass spectrometer (Model QMG420). Samples (200–300 mg) have been heated to 1073 K in He (99.996%) or Ar (99.996%), at a rate of 10 K/min.

Temperature programmed reduction (TPR) experiments have been carried out in an instrument described in detail elsewhere (*16*), using a thermal conductivity detector. Samples (≈0.5 g) were heated in H_2 (5 vol%)/Ar to 873 K at a rate of 10 K/min.

Catalytic Tests

Catalytic tests have been performed in a continuous flow microreactor. A catalyst quantity of 0.4–1 g (50- to 150-μm sieve fraction) was embedded between glass beads (0.5 mm diameter) and glass wool in an 8-mm i.d. glass reactor tube.

Nitrogen (99.999%), hydrogen (99.995%), and standard reactant gas mixtures (5000 ppm CO in nitrogen, 5000 ppm O_2 in nitrogen, and 3650 ppm CO_2 in nitrogen) have been obtained from Pangas. When appropriate, gases were freed from oxygen by passing the corresponding flow through an oxygen adsorption column (OXI-SORB, Messer Griesheim). Flow rates were ad-

justed by mass flow controllers (Brooks, Model 5850 TR).

Prior to the activity tests, the catalysts were exposed to a flow of 1 vol% H_2 in N_2 at 523 K for 5 h. Subsequently, the hydrogen concentration was increased stepwise to 100% within 30 min. The flow was then switched to the desired mixture of reactant gases, as specified below. Typical CO feed rates were adjusted to a value of 1.9×10^{-7} mol s^{-1} g_{cat}^{-1}, or else to 1.4×10^{-6} mol s^{-1} g_{cat}^{-1} in experiments with a large excess of oxygen; space velocities corresponded to 6910 ± 670 h^{-1} and $37{,}500 \pm 3800$ h^{-1}, respectively.

After passing through the microreactor, CO and CO_2 concentrations in the flow were determined by an IR gas analysis instrument (Maihak, Model UNOR 6).

Spectroscopic Measurements

DRIFT experiments have been performed in an environmental chamber (Spectra-Tech, Model 0030-100) equipped with CaF_2 windows and placed into the diffuse reflectance accessory (Spectra-Tech, Model 0030-033) of an FTIR spectrometer (Model 1710, Perkin–Elmer). The chamber was connected to a gas dosing system by 1/16-in. stainless steel tubes. Temperature was controlled by an electrical heating/water cooling system. The gases, CO (purity 99.997%), N_2 (purity 99.999%), and H_2 (purity 99.999%), were obtained from Linde and used without further purification. Oxidations were carried out in a stream of air from which water vapor and CO_2 had been removed by standard adsorption techniques; this medium is referred to as "purified air" in the following.

Unless otherwise stated, the diffuse reflectance spectra (R) observed under reaction conditions were referenced to the background spectrum (R_0), recorded on the unloaded catalyst surface prior to the catalytic experiments. Changes occurring as a function of time or as a consequence of altered conditions will be highlighted by presenting ratios of two subsequently recorded spectra. If a species present on the surface during the recording of spectrum R_1 has desorbed prior to the recording of spectrum R_2, then the ratioed spectrum R_2/R_1 will exhibit a positive-going peak. The changes displayed in the figures have been calculated in this manner.

TABLE 1

Textural Properties of Investigated Catalysts

Sample	BET surface area (m^2 g^{-1})	Pore volume (cm^3 g^{-1})	Mean pore diameter (nm)
Cu/ZrO_2 10 mol%	218	0.15	2.7
Ag/ZrO_2 10 mol%	180	0.18	4.0
Au/ZrO_2 10 mol%	190	0.22	4.6
Au/ZrO_2 1 wt%	158	0.15	3.7
Au/ZrO_2 1 wt% after catalysis	167	0.15	3.7

RESULTS

Structural Properties of the Catalysts

Textural data have been determined for a 50- to 150-μm sieve fraction of the catalyst samples, calcined at 623 K for 5 h. Results are summarized in Table 1. The BET surface areas of the three catalyst containing 10 mol% of Group IB metal differ by no more than 10%, which is within the error of the BET determination. The lower specific surface area of the sample containing 1 wt% of Au is attributed to a higher contribution of crystalline ZrO_2 in the support (see below).

All samples exhibited type IV adsorption/desorption isotherms and type H4 hysteresis loops according to the IUPAC nomenclature (*17*). The samples are mesoporous, with pore diameters ranging from 2 to 50 nm; mean pore diameters are included in Table 1. The shape of the hysteresis loops is indicative of the presence of slit-like mesopores. The micropore volume is zero for all catalysts within experimental accuracy.

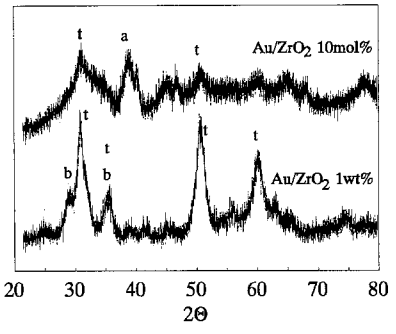

FIG. 1. X-ray diffractogram of calcined Au/ZrO_2 catalysts containing 10 mol% and 1 wt% of gold, respectively.

The crystallization of the zirconia matrix induced by temperature increase has been monitored by *in situ* X-ray diffraction experiments. The as-prepared Au/ZrO_2 catalyst precursors are X-ray amorphous. Indications of partial crystallization appear only at temperatures above 623 K. In Fig. 1, the X-ray diffractograms of two samples that have been calcined under identical conditions (5 h at 623 K) are compared. For the sample containing 1 wt% of Au, strong reflections due to the tetragonal (t) and monoclinic (b) modifications of ZrO_2 are visible. Note that for the sample containing 10 mol% Au the reflections of tetragonal zirconia are much broader, indicating a lower degree of crystallinity. The gold component appears to stabilize the amorphous state of the zirconia. From the line broadening of the characteristic gold reflection (a) at $2\Theta = 38.4°$, a mean gold crystallite size of 4 nm has been estimated using the equation of Warren (*15*).

This result is confirmed by thermal analysis. If the Au (10 mol%)/ZrO_2 catalyst (subsequent to calcination at 623 K) is heated in the DTA apparatus, a strong exothermic signal originating from the crystallization of zirconia is detected at 698 K (Fig. 2). This exotherm is absent in an analogous experiment carried out with the Au (1 wt%)/ZrO_2 sample, which shows that in the catalyst containing only 1% Au, crystallization has occurred already during calcination. In addition, endothermic processes are visible in Fig. 2 from a broad peak extending from 323 to 473 K; mass spectrometry shows that in this temperature range H_2O and CO_2 are desorbing. Either the methanol used in the preparation or else atmospheric CO_2 could be identified as the carbon source, as will be discussed below in connection with the deactivation behavior.

Catalytic Properties

The catalytic activity for CO oxidation as a function of temperature has been tested for a series of metal/zirconia catalysts under identical conditions. The feed contained the reactants, CO and O_2, at concentrations of 2500 ppm each in nitrogen as a carrier gas; a feed rate of 1.90×10^{-7} mol s^{-1} g_{cat}^{-1} has been chosen. In the series of (Group IB metal)/ZrO_2 catalysts, the system containing gold proved to be most active for CO oxidation; the activity decreased in the sequence Au > Ag > Cu. For the fresh catalysts, initial rates may be characterized by the temperatures corresponding to 50% conversion, under the conditions specified. For the catalysts containing 10 mol% of metal, these temperatures have been determined

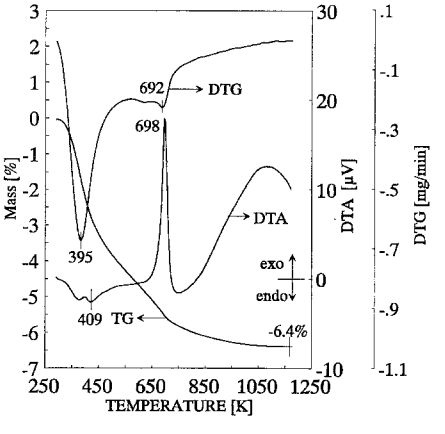

FIG. 2. Thermal analysis of an Au (10 mol%)/ZrO_2 catalyst. The results of simultaneous thermal gravimetry (TG), differential thermal gravimetry (DTG), and differential thermal analysis (DTA) measurements are presented; 200 mg of catalyst was heated in a (sealed) aluminum pan at a rate of 10 K min^{-1}.

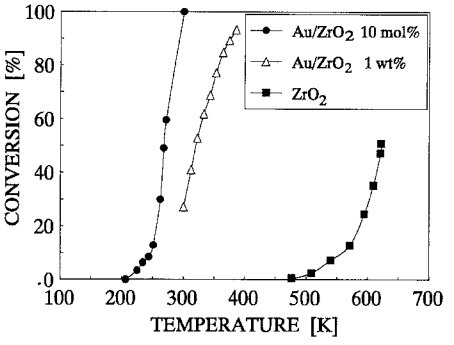

FIG. 3. CO oxidation activity of Au/ZrO_2 catalysts containing 10 mol% (circles) and 1 wt% of gold (triangles), and of the ZrO_2 support (squares). The reactants, CO and O_2, were fed to the catalyst at a concentration of 2500 ppm each in nitrogen, at a rate of 1.9×10^{-7} mol s^{-1} g_{cat}^{-1}; fractional CO conversion is plotted on the abscissa.

to be 268 K for Au, 338 K for Ag, and 398 K for Cu. The corresponding plots of conversion versus temperature for two Au/ZrO_2 catalysts are shown in Fig. 3. The 10 mol% Au/ZrO_2 catalyst would provide complete oxidation of the CO contained in the feed at room temperature. For the sample containing 1 wt% of Au, the temperature corresponding to 50% conversion is 320 K.

Unfortunately, the Au/ZrO_2 catalysts are subject to severe deactivation upon prolonged exposure to CO oxidation conditions. Typically, a decrease of CO conversion by a factor of 3 to 4 was observed over a period of 20 h, depending on pretreatment conditions. To quantify this effect, several experiments have been performed. A reductive pretreatment in hydrogen (2 vol% in N_2) resulted, after switching to CO oxidation conditions, in a decrease of the initial CO oxidation rate, compared to a catalyst pretreated in pure nitrogen. Both catalyst approached the same deactivation time dependence after $\approx$10 h (curve not shown).

In a further series of tests, the catalyst was first heated to 523 K in pure N_2 during 2 h. Subsequently, the catalyst was exposed to CO, CO_2, or O_2 (2500 ppm in nitrogen, flow rate 2 ml s^{-1} g_{cat}^{-1}) at 373 K for 3 h. Thereafter, the feed was switched to reaction conditions (2500 ppm each of CO and O_2 in N_2, mass flow rate 1.9×10^{-7} mol s^{-1} g_{cat}^{-1}, T = 373 K), and the CO_2 conversion was monitored as a function of time. These results are summarized in Fig. 4. The measured integral conversion was converted into an average CO_2 production rate $r_{CO_2,avg}$, which represents an average over the catalyst bed. From Fig. 4 we see that pretreatment in pure nitrogen, which is included for comparison, results in the smallest initial activity and the most extensive deactivation over a period of 10 h. Pretreatment in CO, CO_2, or O_2 results in comparable initial activities; in the case of CO_2 pretreatment, the somewhat higher initial activity is caused by CO_2 desorption in the first period of the experiment. The time dependence of deactivation is similar for these three pretreatments. If deactivation had been due to adsorption of either of the pure molecular gases CO, CO_2, or O_2, one would expect a significantly lower initial activity in one of the three experiments. As Fig. 4 shows that this is not the case, we conclude that the deactivation process occurs mainly due to the simultaneous presence of the reactants, CO and O_2, in the feed. Support for this picture emerges from a careful IR-spectrometric monitoring of the carbon balance in each experiment. Some loss of car-

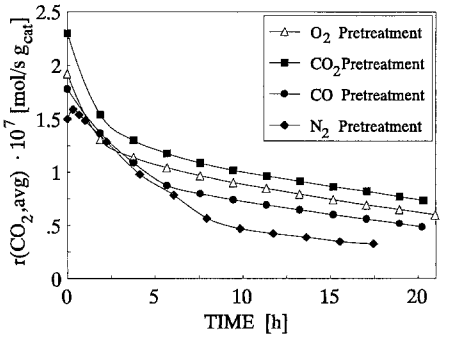

FIG. 4. Deactivation of a Au (1 wt%)/ZrO_2 catalyst under the CO oxidation conditions specified in Fig. 3, at T = 373 K. Symbols refer to different catalyst pretreatments, as described in more detail in the text.

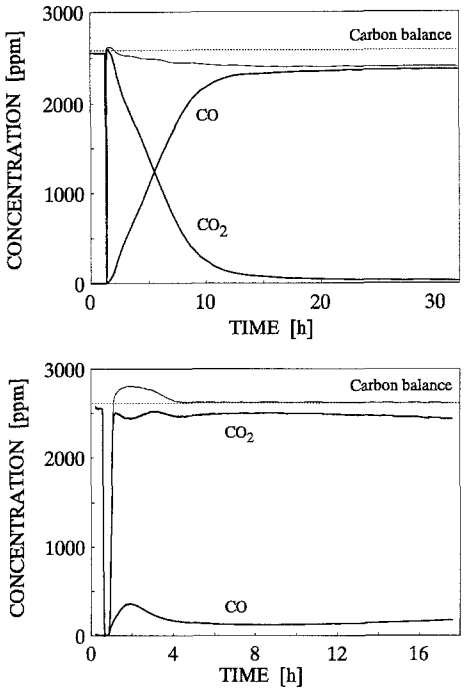

FIG. 5. Time dependence of CO oxidation activity at 373 K of a Au (1 wt%)/ZrO_2 catalyst, monitored by recording the intensities of CO and CO_2 mass signals. The $[O_2]/[CO]$ concentration ratio was set to values of 40 (top) and of 0.5 (bottom), respectively. For each case, the carbon balance, i.e., the sum of the CO and CO_2 intensities, is shown as the topmost trace.

bon (typically, ≈5%) is observed for each run, which points to deactivation by some carbonaceous deposit on the catalyst surface. This point is addressed more fully below.

It is illustrative to investigate the influence of the O_2 partial pressure during reaction on the deactivation behavior. In Fig. 5, CO_2 conversion over a 1 wt% Au/ZrO_2 catalyst is monitored in the presence both of a large oxygen excess ($[O_2]/[CO]$ = 40) and of a stoichiometric reaction mixture ($[O_2]/[CO]$ = 0.5). Rapid deactivation is observed in excess oxygen, and the carbon balance is negative (Fig. 5). In contrast, the catalyst stays fully active in a stoichiometric reaction mixture, and the carbon balance (sum of CO and CO_2 concentration) is constant at 100% after an initial release of additional carbon during the first 3 h. The conditions under which most of the catalytic activity tests have been run ($[O_2]/[CO]$ = 1, corresponding to a twofold stoichiometric excess) represent an intermediate case. Average CO_2 production rates for these three catalytic runs are summarized in Fig. 6. The fact that the presence of excess oxygen results in fast deactivation, whereas no deactivation is observed for a stoichiometric reaction mixture, points to an oxygenated carbon species covering the surface.

To detect the species responsible for deactivation, thermal desorption experiments combined with mass spectrometric analysis of the desorbed products have been performed with a deactivated catalyst sample (Fig. 7). Three separate weight losses can be recognized in the differential thermal gravimetry (DTG) curve. The mass loss between 323 and 473 K is associated with the desorption of H_2O and CO_2, as was found for the catalyst precursor (Fig. 2). Some further water is also released during the crystallization of the zirconia component at 712 K. CO_2 desorption continues from 673 to 873 K. Most relevant to the deactivation is the DTG peak at 526 K, which is absent on

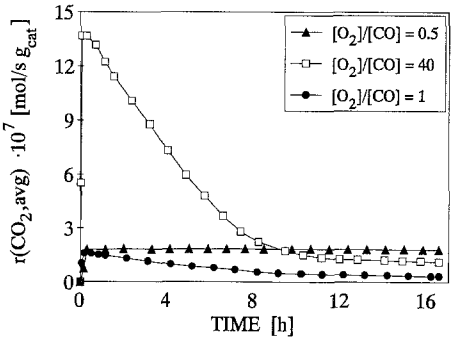

FIG. 6. Comparison of CO oxidation activity and time dependence of deactivation for different oxygen partial pressures. The catalyst {Au (1 wt%)/ZrO_2} was exposed to a CO feed of 1.9×10^{-7} mol s^{-1} g_{cat}^{-1} for the experiments carried out with $[O_2]/[CO]$ = 0.5 (triangles) and 1.0 (circles). In the experiment with $[O_2]/[CO]$ = 40 (squares), the CO feed was 1.4×10^{-6} mol s^{-1} g_{cat}^{-1}. The CO concentration in nitrogen was 2500 ppm in all experiments.

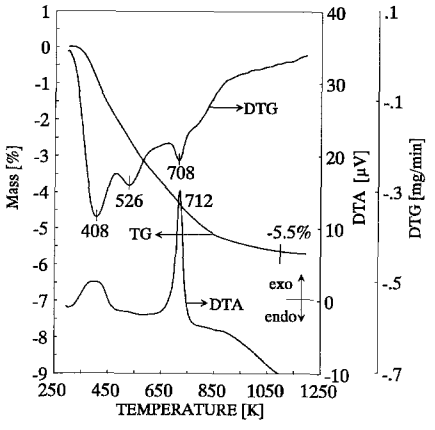

FIG. 7. Thermal analysis of a Au (1 wt%)/ZrO_2 catalyst deactivated under CO oxidation conditions ([O_2]/[CO] = 1). Abbreviations and experimental parameters are the same as in Fig. 2.

samples not exposed to catalytic reaction conditions. This peak is associated with the masses m/e = 27, 29, 30, 32, 41, and 43. The detection of these masses is astonishing, as they are usually associated with organic species of the type C_2H_3, C_2H_5, C_3H_5, and C_3H_7. Oxygenated species, such as HCO (m/e = 29), H_2CO (m/e = 30), and H_3C_2O (m/e = 43), could contribute as well to the observed masses.

The quantity of CO and CO_2 desorbed from a deactivated catalyst can be correlated with the loss of carbon registered when recording the carbon balance during the catalytic run. A deactivated catalyst sample was heated to 873 K in nitrogen in the CO oxidation apparatus. The integrated quantity of CO and CO_2 desorbed during this temperature program corresponded to 1.5–2% of the catalyst weight. On the other hand, a carbon loss of 100 ppm during a 20-h catalytic run at a feed rate of 100 ml min^{-1} g_{cat}^{-1} would correspond to a mass increase of 2–3%, in very satisfactory agreement with the desorbed quantity.

It is worthwhile to emphasize (cf. Table 1) that the texture of the catalyst samples did not change during the catalytic runs. XRD measurements performed after catalysis confirmed that the degree of crystallinity of the zirconia, as well as the gold particle size, remained unchanged as well.

Diffuse Reflectance FTIR Experiments

In a first experiment, a catalyst sample (10 mol% Au/ZrO_2) was initially exposed to pure CO at a static pressure of 2 bar at room temperature. Then the gas atmosphere was flushed with purified air, and diffuse reflectance (DRIFT) spectra of the surface were recorded as a function of time (Fig. 8). The bottom spectrum shows the presence of surface-bound carbonates [bidentate: shoulders at 1680 and 1256 cm^{-1} (*18*); monodentate: 1426 cm^{-1} (*19*)], surface formate [1593 and 1374 cm^{-1} (*18, 20, 21*)], and adsorbed CO [bridge bonded: 1992 cm^{-1}; linearly bonded: 2130 cm^{-1} (*6, 18, 22, 23*)]. There is a weak residue of desorbing gaseous CO (doublet centered at 2150 cm^{-1}), and a stronger peak due to desorbing CO_2 product. A spectrum recorded after 15 min of continuous air flushing (not shown) exhibits the same spectral features, with altered intensities. The CO surface peak at 2130 cm^{-1} is more clearly recognized after gaseous CO has been completely purged. In the upper half of Fig. 8, we present the difference between a spectrum recorded after 4 h of air flushing and the bottom spectrum. One recognizes that the surface concentrations of carbonates and CO (ads) have decreased, whereas the formate concentration has *increased*. Surface-bound CO and gaseous CO_2 continue to be released from the surface in detectable amounts for 2 h after the beginning of air flushing.

CO oxidation experiments over Cu/ZrO_2 and Pd/ZrO_2 catalysts are shown in Fig. 9 for comparison. On the Cu/ZrO_2 catalyst, specified in the experimental section, strong carbonate signals are exposed in the background spectrum recorded prior to any exposure to CO oxidation conditions (Fig. 9a, bottom spectrum). This catalyst was exposed to an atmosphere of CO at room temperature and a pressure of 2 bar for 30 min. Formation of adsorbed CO (2010 cm^{-1}, dou-

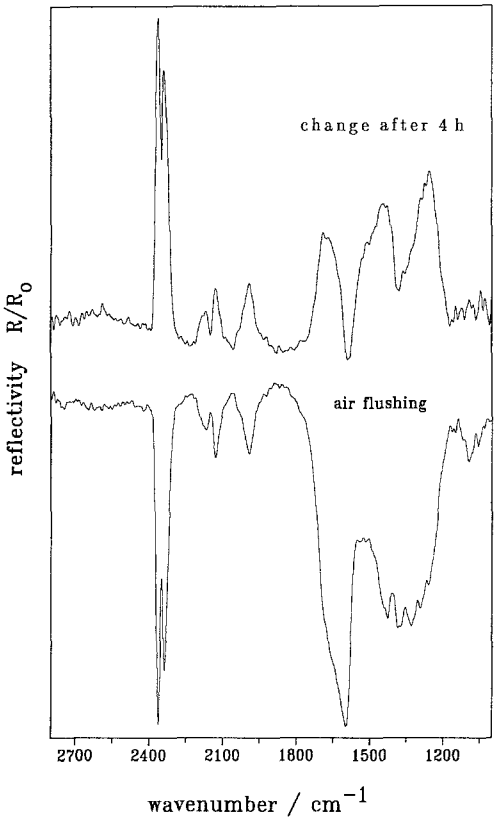

FIG. 8. *In situ* FTIR spectra recorded over a Au (10 mol%)/ZrO_2 CO oxidation catalyst. The diffuse reflectance spectrum, R, is referenced with respect to the background spectrum R_0 recorded on the catalyst surface prior to the experiment. The catalyst was loaded by exposure to 2 bar of CO at room temperature; the lower trace represents the first spectrum recorded immediately after purging the cell with purified air. Time-dependent changes during continued flushing with purified air were monitored thereafter. The upper trace represents the ratio between a spectrum recorded 4 h after the start of air flushing and the first spectrum.

blet) and carbonate, but no gaseous CO_2, was detected. These features are clearly observed after air flushing (Fig. 9a, middle trace). Only after heating in air to 473 K the formation of CO_2 (g), a decrease in adsorbed CO and carbonates, and an increase in surface formate bands are noticed (Fig. 9a, top trace).

This sequence of events is analogous to the one observed with Au/ZrO_2; however, CO oxidation activity sets in only at considerably higher temperatures, in agreement with the activity comparison mentioned above. The Au/ZrO_2 catalyst exhibits a high initial activity followed by severe deactivation. The Cu/ZrO_2 system exhibits a lower activity, and deactivation is less severe. The latter system is covered by large amounts of carbonates from the beginning. The presence of abundant carbonate on the active Cu/ZrO_2 catalyst points to the fact that surface carbonate does not represent the deactivating species.

An analogous experiment performed over a Pd (5 wt%)/ZrO_2 catalyst is presented in Fig. 9b for comparison. In the background spectrum of the unloaded catalyst (bottom), surface-bound formate is recognized. Dominant surface species observed after air flushing are bridge-bonded CO [1928 cm^{-1} (*18, 24*)], linearly bonded CO [1984 cm^{-1} (*18, 24*)], and much weaker signals due to carbonates (1660 cm^{-1}) and formate (1570, 1375 cm^{-1}). After 45 min, surface-bound CO is observed to decrease. We note that formate signals are decreasing, whereas carbonate signals are *weakly* increasing with time; this is seen from the negative going peak at 1660 cm^{-1}, and the downward broad bands at 1440 and 1264 cm^{-1} (*18*). This behavior of Pd (5 wt%)/ZrO_2 is opposite to the one observed with Au/ZrO_2.

The experiment shown in Fig. 10 is complementary to that presented above in Fig. 8. After loading the catalyst surface with CO at $p = 2$ bar at room temperature, the *in situ* cell was flushed with nitrogen (rather than with air as used in Fig. 8) and heated to 573 K for 30 min, and the spectrum shown in the lower trace of Fig. 10 was recorded. Subsequently, the sample was cooled again to room temperature under nitrogen. The middle trace in Fig. 10 presents the difference between the two spectra recorded before and after the entire cycle described; an increase in formate (1590, 1380 cm^{-1}) and a decrease in surface carbonate species (1680, 1280 cm^{-1}) are recognized. Formation of linearly bonded CO on gold [2110 cm^{-1} (*6,*

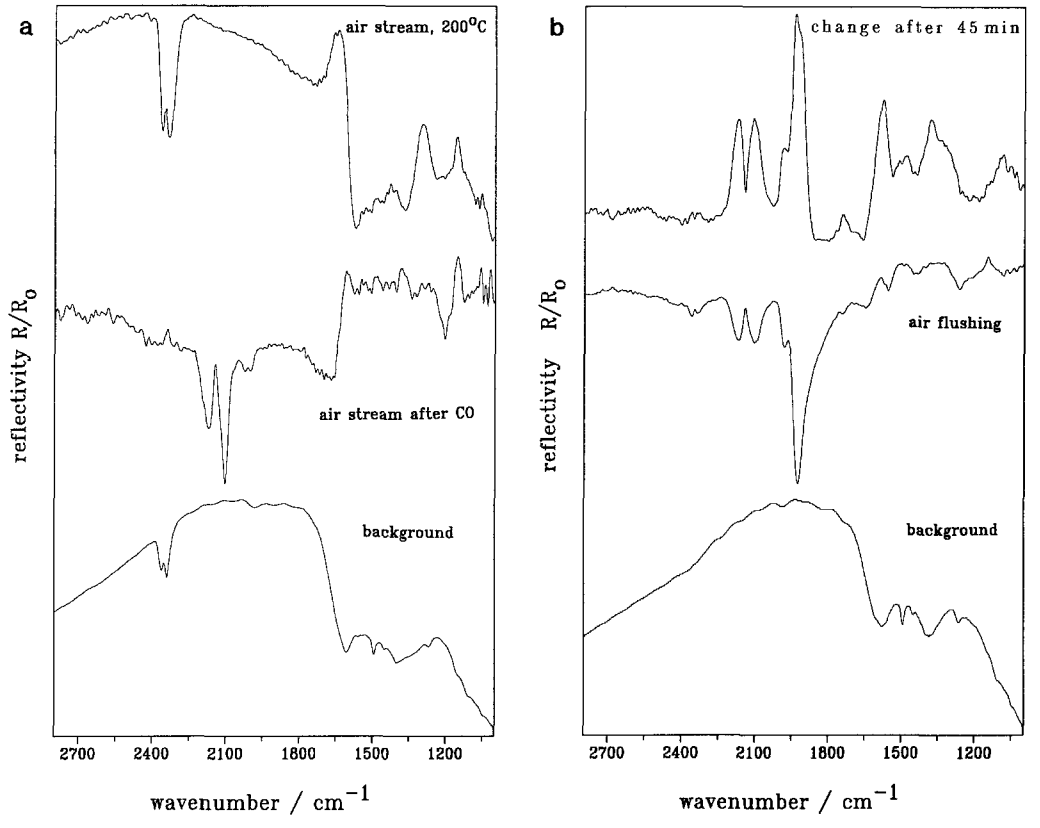

FIG. 9. CO oxidation over Cu/ZrO_2 (a) and Pd/ZrO_2 (b) catalysts. In the bottom trace of (a), the background diffuse reflectance spectrum of the Cu/ZrO_2 catalyst prior to exposure to reaction conditions is presented, as referenced to a totally reflecting mirror surface. The catalyst was then loaded with CO (2 bar, room temperature), the cell was purged with purified air, and the middle spectrum was recorded; this spectrum is ratioed with respect to the background spectrum of the unloaded catalyst. The top spectrum shows the changes induced by heating this catalyst to 473 K under a stream of purified air. For the Pd/ZrO_2 catalyst (b), species present on the surface prior to exposure to reaction conditions are visible in the background spectrum shown in the bottom trace, which is again referenced to a mirror surface. After loading the catalyst by exposure to 2 bar of CO at room temperature followed by air purging, the middle spectrum was recorded. Time dependent changes that are occurring during continued air flushing at room temperature are demonstrated by the difference spectrum recorded after 45 min (top trace).

18, 19, 23)] and of zirconia-bound CO (2217 cm^{-1}, see below) are observed. The latter spectrum has been used as a new reference, to record the changes induced by CO adsorption onto the current surface state of the catalyst. An increase in carbonate bands was registered (spectrum not shown). When the cell is flushed by air, the formate species disappears, the concentration of surface CO decreases, and more carbonate is formed.

In the experiment just described, CO_2 is produced in the absence of oxygen in the gas feed. It therefore appeared important to investigate whether the oxygen required for CO_2 formation was supplied from the surface (and/or bulk) of the catalyst, or whether it was produced by CO dissocation, i.e., a disproportionation reaction of the reactant. To clarify this question, the same catalyst sample was subjected to several successive

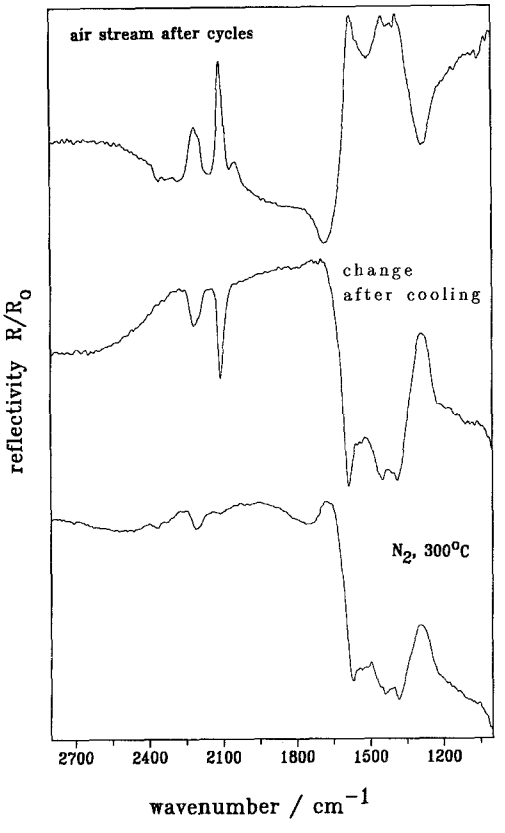

FIG. 10. Reactions occurring on the surface of a Au (10 mol%)/ZrO_2 catalyst subsequent to CO exposure, in the absence of oxygen. The bottom spectrum was recorded after loading the catalyst with CO (1 bar) at room temperature, purging with nitrogen, and heating to 573 K, where the sample was held for 30 min. After cooling back to room temperature, another spectrum was recorded; the middle trace represents the difference between the spectra taken before and after the entire cycle. This sequence of CO adsorption, heating in nitrogen, and cooling was repeated five times. Thereafter, the cell was flushed with purified air, and the top spectrum was recorded.

cycles of CO adsorption at room temperature (2 bar, 15 min), flushing with nitrogen, heating, holding at 573 K under nitrogen, and cooling again to room temperature. In the first cycle following the experiment described in the preceding paragraph, comparable results were obtained. An increase of surface formate and a small increase of carbonate were observed under CO loading. After N_2 flushing, only CO(ads) and formate remained visible. Heating of the cell resulted in a decrease in carbonate (due to CO_2 desorption) and an increase in formate at the expense of adsorbed CO. After cooling back to room temperature, the overall effect of the cycle was a decrease in carbonate and an increase in formate as well as adsorbed CO (2110 and 2217 cm^{-1}).

In the next cycle, the only perceptible change in adsorbate concentrations during CO loading was an increase in the carbonate coverage. However, the overall result of the cycle was the same as found in the previous one, i.e., a decrease in carbonate and an increase in CO(ads) and formate. Changes became smaller in subsequent cycles, indicating that no more surface carbonate was available, and that the binding sites for CO and formate were occupied.

When the cell was subsequently flushed with purified air, the oxidation of surface CO yielding CO_2 was observed, accompanied by a decrease of surface formate and an increase in surface carbonate species (Fig. 10, upper trace). We note that this behavior is different from the one of a *fresh* catalyst observed upon air exposure after CO loading (Fig. 8).

Hydrogen reduction of the catalyst surface has been probed as an alternative to CO reduction described in the preceding paragraph. The most significant change recorded after exposure to a stream of pure hydrogen (2 $dm^3\ h^{-1}$) at 473 K for 45 min is the disappearance of surface carbonates (Fig. 11, lower trace). When this surface is exposed to CO again, some carbonate is reformed (middle trace); this process is strongly enhanced when purified air is admitted to the catalyst sample (top trace).

At this point, it is important to assess which species are formed on the surface upon exposure to the oxidation product, CO_2. A catalyst sample was exposed to a static CO_2 pressure of 1 bar at room temperature (Fig. 12, lower trace), a stream (3 $dm^3\ h^{-1}$) of CO_2 at 473 K, and a flow of CO_2 (50 vol%)/air at $p = 1.4$ bar at room tempera-

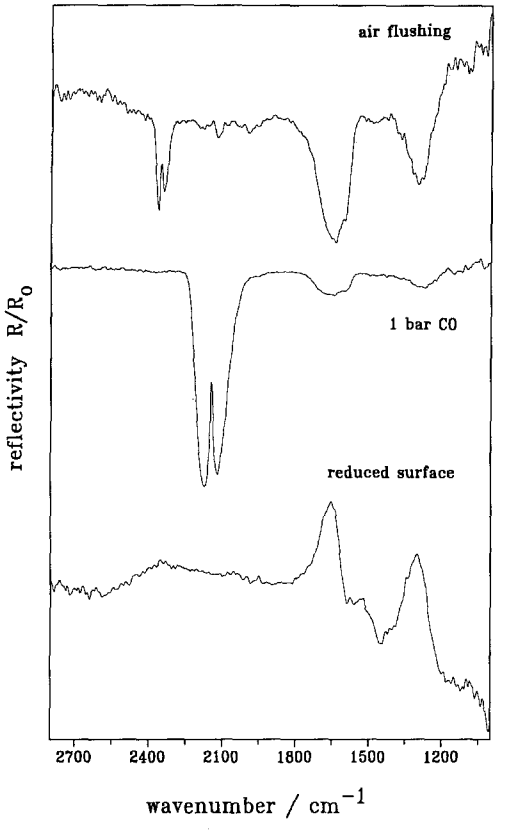

FIG. 11. Hydrogen reduction of a Au/ZrO_2 catalyst. The bottom trace shows the difference spectrum between the reduced and the untreated states of the catalyst surface. The results of CO adsorption (2 bar) onto the reduced catalyst are presented in the middle trace. After subsequent flushing with purified air, the top spectrum was recorded (background: reduced catalyst).

ture. Surface carbonates (>1630, 1442, and 1230 cm^{-1}) dominate the spectrum in a pure CO_2 atmosphere (bottom); the formate concentration (1583 and shoulder at 1370 cm^{-1}) is higher at elevated temperature and under CO_2/air atmospheres (middle and upper spectra). We note that no CO (g) is produced. A band observed at 1710 cm^{-1} (middle and upper traces of Fig. 12) might be assigned to a surface formyl species (*25*).

In a final experiment, CO adsorption on Au/ZrO_2 and adsorption on the pure ZrO_2 support were compared to differentiate between the CO species bonded to the gold particles and to the support material, respectively. In particular, the weak signal at 2220 cm^{-1} detected in Fig. 10 after heating a CO-loaded surface to 573 K in nitrogen remained to be identified. When Au/ZrO_2 is loaded with CO and then flushed with nitrogen *at room temperature* (Fig. 13, lower trace), bridged and linearly bonded CO are detected at 1983 and 2110 cm^{-1}, respectively. On the ZrO_2 support, the analogous room temperature experiment yields a band at 2000 cm^{-1} (middle trace). (Signals above 2000 cm^{-1} are due to gaseous CO and CO_2, respectively.) Only after heating to 573 K is the 2220 cm^{-1} feature observed on pure ZrO_2 (top trace). If we compare this experiment with the one described above (Fig.

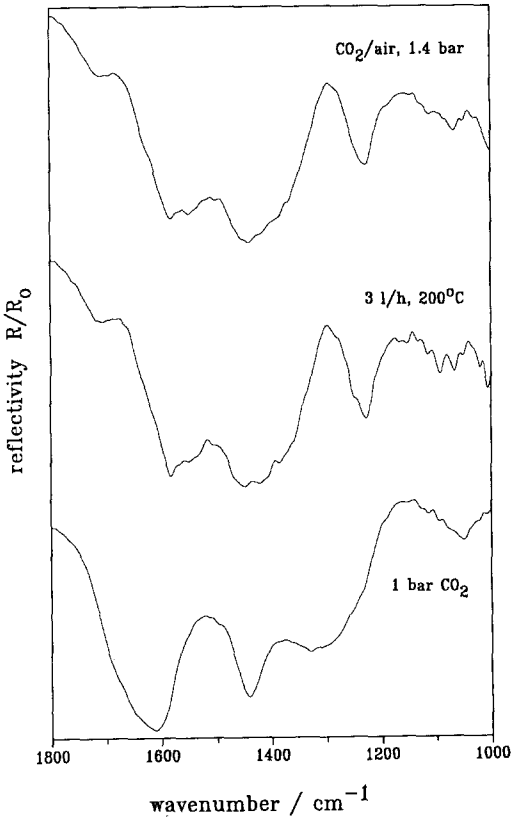

FIG. 12. CO_2 adsorption onto a Au/ZrO_2 catalyst studied by DRIFT spectroscopy. The lower trace was recorded at room temperature and a CO_2 pressure of 2 bar. The middle spectrum was obtained in a flow of CO_2 (3 dm^3 h^{-1}) at 473 K. For the top spectrum, the catalyst was exposed to a flow of CO_2 (50 vol%)/air at p = 1.4 bar and room temperature.

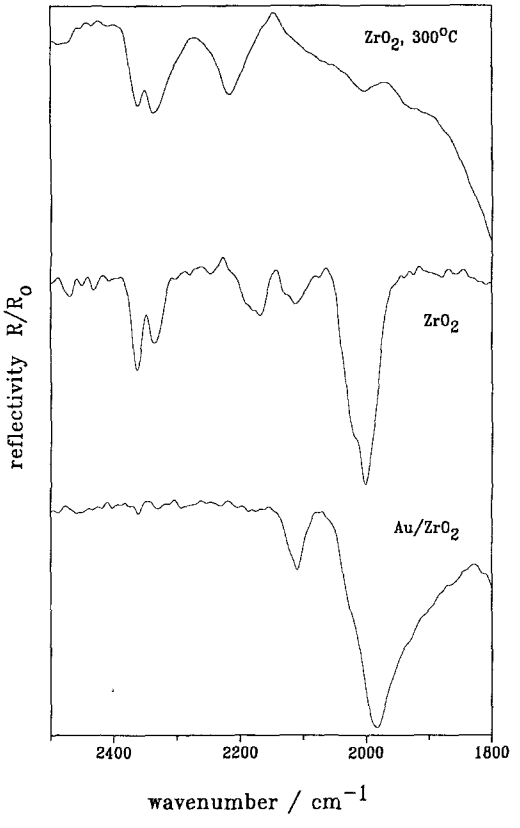

FIG. 13. Comparison of CO adsorption onto Au/ZrO_2 and onto the ZrO_2 support. The spectrum recorded over Au/ZrO_2 after CO loading (2 bar) and nitrogen flushing at room temperature is shown in the bottom trace. The middle spectrum was obtained on the ZrO_2 support subject to the same treatment. After the latter surface had been heated to 573 K in nitrogen (cf. Fig. 10), the top spectrum was recorded.

10), we can attribute the 2110 cm^{-1} band to linearly bonded CO on gold, and the 2220 cm^{-1} to CO adsorbed on ZrO_2. The intensive feature corresponding to bridge-bonded CO appears at slightly different frequencies on Au/ZrO_2 (1983 cm^{-1}) and on ZrO_2 (2002 cm^{-1}); it may thus comprise CO surface species bonded both to the gold particles and to the zirconia support.

DISCUSSION

The deactivation behavior of the highly active Au/ZrO_2 catalysts, and its dependence on the O_2/CO feed ratio, can be understood in light of changes occurring in the adsorbed surface layer during exposure to reaction conditions.

At first sight, it seems difficult to interpret the changes in surface concentrations observed under a variety of experimental conditions, as reported above in Figs. 8–13. In particular, it is remarkable to note that the formate coverage is observed to *increase* again when purified air is passed over a fresh catalyst surface that has been loaded with CO (Fig. 8). This apparent complexity arises from the fact that the catalyst surface, in particular in a flowing system, represents an open system; addition of reactants (CO, O_2) and removal of products (CO_2, H_2O) results in shifts in a chain of interconnected equilibria on the surface. Furthermore, there is evidence that the catalyst surface can be prepared in either an oxidized state, with a reservoir of adsorbed surface oxygen (O_s) available for oxidation processes, or a reduced state, which is devoid of surface oxygen.

An additional point of importance for the discussion is the initial coverage of surface species present on the catalyst surface before exposure to CO oxidation conditions. A Pd/ZrO_2 catalyst stored under ambient conditions is loaded with surface formate species (Fig. 9b). On Au/ZrO_2, carbonate is present, which is reduced by hydrogen at elevated temperatures (Fig. 11). An even higher concentration of carbonate is detected on the Cu/ZrO_2 sample (Fig. 9a).

The changes observed in the FTIR spectra can be interpreted in terms of a reaction scheme that incorporates these two states of the surface, and is shown in Fig. 14. For the sake of clarity, the various forms of adsorbed CO species present on the catalyst surface are not shown explicitly in the schematic representations of the respective surface states; adsorbed CO is however involved in several of the transformations between the states. The experiments reported above in Figs. 8–13 will now be discussed in sequence by reference to Fig. 14.

The surface of the as-prepared Au/ZrO_2 catalyst, which has been stored under ambient conditions, is equilibrated with atmo-

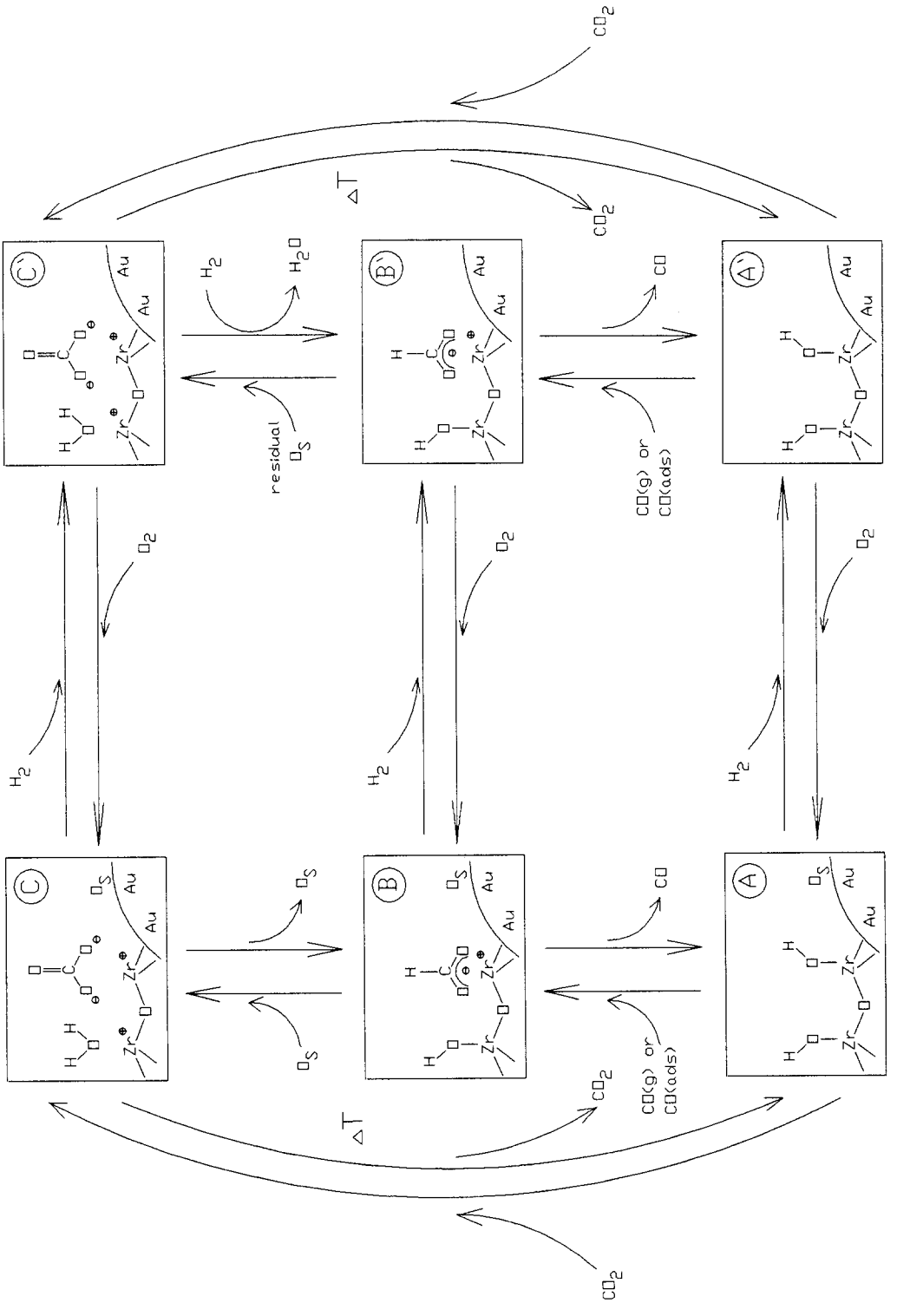

FIG. 14. Proposed reaction for CO oxidation over Au/ZrO_2. Left and right sides of the diagram correspond to oxidized and reduced states of the catalyst surface, respectively. Note that oxygen adsorption from the gas phase, and the stoichiometry of oxygen (O_s) consumption, are not explicitly displayed. The scheme is discussed in detail in the text.

spheric oxygen (left-side states in Fig. 14). When CO is admitted to an empty site {(A)} on this surface (Fig. 8), formate is formed by insertion of CO into a surface hydroxyl group {(A) → (B)}. This reaction is accompanied by a decrease in the OH stretching absorption of hydroxyl groups of the zirconia support (spectral region not shown).

Formate is oxidized by the available surface oxygen to yield carbonate {(B) → (C)}. When the catalyst surface loaded in this way is flushed with purified air (Fig. 8), the connected equilibria are shifted in such a way that CO_2 is desorbed from surface carbonate {(C) → (A)}. The increase in surface formate observed under these conditions is explained by the fact that adsorbed CO, which is stored on the catalyst surface, reenters {(A) → (B)} the sites that have been freed by CO_2 desorption. The formate species (B) accumulates on the surface in large concentrations in the presence of excess oxygen and appears to be very stable. Extensive site blocking by this species is suggested to be responsible for the catalyst deactivation observed for large $[O_2]/[CO]$ reactant ratios. We cannot exclude the possibility that the deactivation is accompanied by some restructuring of the surface as well.

The experiment reported in Fig. 10, where CO adsorption is followed by a nitrogen purge, is discussed next. Carbonate formation in the absence of oxygen supply from the gas phase gradually depletes the catalyst of surface oxygen {state (C'), and reaction cycle (C') → (A') → (B') → (C')}.

A temperature increase to 573 K in nitrogen results in CO_2 desorption {(C') → (A')}. Adsorbed CO reenters {(A') → (B')} the sites vacated by CO_2 desorption, and an increase of surface formate is observed (Fig. 10, bottom trace). When CO is admitted to this reduced surface state (B') of the catalyst, the series of interconnected equilibria is shifted by the massive increase of the CO concentration; some carbonate appears to be formed by the reaction of formate with residual surface oxygen {(B') → (C')}.

When several successive cycles of CO adsorption and heating under nitrogen are carried out, the concentration of carbonates is continuously diminished by CO_2 desorption {(C') → (A')}. Obviously, the oxygen required for carbonate formation {(B') → (C')} cannot be replenished from the CO feed. After the limited supply of absorbed oxygen, stored on the surface or in the subsurface region, has been exhausted, the available binding sites are covered by formate and adsorbed CO {state (B')}.

Upon admission of air to the catalyst surface at this stage, surface oxygen is replenished, and carbonate is formed again {sequence (B') → (B) → (C)}. Subsequently, CO_2 is produced by the catalytic reaction pathway (C) → (A) → (B) → (C) until the adsorbed CO is consumed (Fig. 10, upper trace).

These experiments may be related to the observation that catalyst deactivation is much less severe at low oxygen partial pressures $\{[O_2]/[CO] = 0.5\}$. In the state (B'), the surface formate species, which are not stabilized by excess oxygen, do not give rise to irreversible site blocking. These less strongly bound surface formate species are readily converted to CO_2 by oxygen from the stoichiometric feed.

Hydrogen reduction of the catalyst (Fig. 11) results in a reduced state of the surface and a reduction in surface carbonate concentration by CO_2 desorption {(C') → (A')}. When CO is admitted to the reduced catalyst surface, the formation of CO(ads) and of carbonate {(A') → (B') → (C')} are observed, but no gaseous CO_2 is formed due to the limited amount of available surface oxygen.

The adsorption of the CO_2 product (Fig. 12) at room temperature mainly results in surface carbonate formation {(A) → (C)}. In addition, some dissociation of surface carbonates appears to occur at elevated temperatures (473 K) or in CO_2/air mixtures, to yield surface oxygen and formate {reaction (C) → (B)}. Formate, in turn, may be thought to be in rapid equilibrium with surface hydroxyl groups and adsorbed CO {(A)}, via surface formyl as an intermediate,

as has been formulated in more detail elsewhere [cf. Fig. 6 of Ref. (25)]. The band observed at 1708 cm^{-1} at 473 K has been tentatively assigned to this surface formyl species.

The presence of various forms of adsorbed CO has been mentioned above in conjunction with Figs. 10 and 13. Bridge-bonded CO species are found to absorb between 1980 and 2000 cm^{-1} under the conditions used, with some indication that the lower limit of this interval corresponds to CO on gold, and the higher limit to CO on zirconia. Linearly bonded CO is detected at $\approx$2100 cm^{-1} on Au/ZrO_2, and at $\approx$2220 cm^{-1} on pure ZrO_2. The latter species is also produced (Fig. 10) upon heating of a reduced, formate-covered surface {state (B′) in Fig. 14}.

At this point, one should be aware of the possibility that the CO_2 product might also be produced from adsorbed CO and gaseous O_2 by an Eley–Rideal mechanism. The present experiments do not provide evidence whether the latter represents an important contribution. The above-mentioned conclusions with regard to the mechanism of deactivation, i.e., the blocking of CO adsorption sites by tightly bound surface formate in the presence of excess oxygen {state (B) of the surface}, would also be consistent with an Eley–Rideal model of the CO oxidation.

Surface species and reaction-induced changes of their respective coverages on the Cu/ZrO_2 catalyst are similar to those observed on Au/ZrO_2, and hence a reaction scheme analogous to the one shown in Fig. 14 may be proposed. The most important difference consists in the fact that CO oxidation takes place at a significant rate only at higher temperatures.

On the surface of Pd/ZrO_2, a high concentration of surface formate is present already before exposure to CO oxidation conditions. More formate is formed upon CO adsorption. CO_2 production in the absence of gaseous oxygen in the feed results only in a minor increase of the carbonate concentration {cycle (B) $\rightarrow$ (C) $\rightarrow$ (A) $\rightarrow$ (B) in the terminology of Fig. 14}. The oxygen required for this reaction is either provided by surface or subsurface oxygen, as discussed in detail elsewhere (26). When air is passed over the CO-loaded catalyst, adsorbed CO is oxidized (27), and formate is converted to carbonate {(B) $\rightarrow$ (C)}; the latter is partly desorbed {(C) $\rightarrow$ (A)}. Due to the availability of subsurface oxygen on Pd, the oxidation of the intermediate formate to carbonate is fast in the "oxidized" state of the catalyst surface, such that no significant surface concentration of formate is maintained.

CONCLUSIONS

Gold catalysts supported on amorphous zirconia exhibit a high initial CO oxidation activity even at room temperature. The initial rate is particularly high after pretreatment in oxygen, by which a high coverage of surface oxygen is established. However, the time-dependent deactivation occurring over a time scale of $\approx$20 min is not significantly changed by the adsorption of O_2, N_2, CO, or CO_2 prior to the catalytic runs. From this observation we conclude that the deactivation is not due to molecular adsorption of either one of these species. Rather, the deactivation depends sensitively on the O_2/CO ratio. For a stoichiometric reaction mixture (O_2/CO = 0.5), the activity remains constant over a period of $\approx$20 h. In the presence of excess oxygen, the initial activity is higher but deactivation is much more severe. This fact, as well as the results of thermal desorption/mass spectrometry experiments on deactivated samples, indicate the presence of an oxygenated carbon species on the deactivated catalyst surface.

When a fresh Au/ZrO_2 catalyst sample is first loaded with CO and subsequently flushed with purified air, the initially high concentration of surface carbonates decreases, whereas the formate is observed to increase. A mechanism has been proposed in which adsorbed CO first reacts with surface hydroxyl groups to yield formates. Formate is oxidized to carbonate by surface oxygen; the cycle is completed by CO_2 desorption.

Replenishment of surface oxygen from the gas phase is slow as a consequence of the intrinsically low sticking probability of O_2. This process, as well as the oxidation of formate to carbonate, appears to be limiting for the overall catalytic turnover frequency.

In reducing atmospheres, carbonate and gaseous CO_2 are produced until the available surface oxygen has been depleted. Thereafter, large quantities of surface formate are formed. When purified air is admitted to this surface, an upsurge of CO_2 production and the formation of carbonates are observed.

In the deactivated state in the presence of excess oxygen {(B) in Fig., 14}, the catalyst surface appears to be covered with a high concentration of surface formate; further reaction from this state is impeded because the required adsorption and/or the reactive sites are blocked. In contrast, when using stoichiometric or reducing reaction mixtures, the catalyst resides in the state (B′) (Fig. 14). Starting from this active state of the surface, the catalytic cycle can proceed, for which the steps of O_2 and CO adsorption, insertion of CO into surface hydroxyl groups to yield formate, formate → carbonate oxidation, and thermally activated CO_2 desorption have been identified from the temperature-dependent FTIR spectra.

ACKNOWLEDGMENTS

The authors are indebted to R. A. Köppel for the preparation of the Cu/ZrO_2 and Pd/ZrO_2 reference samples, to M. Maciejewski for carrying out the thermoanalytical measurements, and to F. Zimmermann for providing the data reduction software. Financial support of this work by the Deutsche Forschungsgemeinschaft (SFB 213) and by the Schweizerische Bundesamt für Energiewirtschaft is gratefully acknowledged.

REFERENCES

1. See, e.g., Engel, T., and Ertl, G., *Adv. Catal.* **28,** 1 (1979); "The Chemical Physics of Solid Surfaces and Heterogeneous Catalysis" (D. A. King and D. P. Woodruff, Eds.), Vol. 4, p. 73. Elsevier, Amsterdam, 1972.
2. Schwank, J., *Gold Bull.* **16,** 103 (1983).
3. Cant, N. W., and Fredrickson, P. W., *J. Catal.* **37,** 531 (1975).
4. Wachs, I. E., *Gold Bull.* **16,** 98 (1983).
5. Shibata, M., Kawata, N., Masumoto, T., and Kimura, H., *Chem. Lett.* 1605 (1985).
6. Dumas, P., Tobin, R. G., and Richards, P. L., *Surf. Sci.* **171,** 579 (1986).
7. Outka, D. A., and Madix, R. J., *Surf. Sci.* **179,** 351 (1987).
8. Haruta, M., Kobayashi, T., Sano, H., and Yamada, N., *Chem. Lett.* **829,** 405 (1987).
9. Haruta, M., Kageyama, H., Kamijo, N., Kobayashi, T., and Delannay, F., *Stud. Surf. Sci. Catal.* **44,** 33 (1989).
10. Haruta, M., Yamada, N., Kobayashi, T., and Iijima, S., *J. Catal.* **15,** 301 (1989).
11. Haruta, M., Kobayashi, T., Iijima, S., and Delannay, F., *in* "Proceedings, 9th International Congress on Catalysis, Calgary, 1988" (M. J. Phillips and M. Ternan, Eds.), Vol. 3, p. 1206. Chem. Institute of Canada, Ottawa, 1988.
12. Lazarov, D., Stancheva, M., and Manev, S., *Izv. Khim.* **20,** 528 (1987).
13. Tarasov, A. L., Przhevalskaya, L. K., Shvets, V. A., and Kazanskii, V. B., *Kinet. Katal.* **29,** 1181 (1988).
14. Gardner, S. D., Hoflund, G. B., Upchurch, B. T., Schryer, D. R., Kielin, E. J., and Schryer, J., *J. Catal.* **129,** 114 (1991).
15. Warren, B. E., *J. Appl. Phys. B* **12,** 75 (1941).
16. Monti, D. A. M., and Baiker, A., *J. Catal.* **83,** 323 (1983).
17. Sing, K. S. W., Everett, D. H., Haul, R. A. W., Moscou, L., Pierotti, R. A., Rouquerol, J., and Siemieniewska, T., *Pure Appl. Chem.* **57,** 603 (1985).
18. Davydov, A. A., "Infrared Spectroscopy of Adsorbed Species on the Surface of Transition Metal Oxides." Wiley, Chichester, 1984.
19. Kiselev, V. F., and Krylov, O. V., "Adsorption and Catalysis on Transition Metals and Their Oxides." Springer, Berlin, 1989.
20. He, M. Y., and Ekerdt, J. G., *J. Catal.* **87,** 381 (1984).
21. Edwards, J. F., and Schrader, G. L., *J. Phys. Chem.* **89,** 782 (1985).
22. Yates, J. T. Jr., and Madey, T. E., Eds., "Vibrational Spectroscopy of Molecules on Surfaces." Plenum, London, 1987, and references cited therein.
23. Chang, S. C., Hamelin, A., and Weaver, M. J., *Surf. Sci. Lett.* **239,** L543 (1990).
24. Lokhov, Y. A., and Davydov, A. A., *Kinet. Catal.* **21,** 1093 (1980).
25. Schild, Ch., Wokaun, A., and Baiker, A., *J. Mol. Catal.* **69,** 347 (1991).
26. Baiker, A., Gasser, D., Lenzner, J., Reller, A., and Schlögl, R., *J. Catal.* **126,** 555 (1990).
27. Barnickel, P., Wokaun, A., and Baiker, A., *J. Chem. Soc. Faraday Trans.* **87,** 333 (1991).